ELSEVIER

Thermochimica Acta 268 (1995) 161–168

thermochimica acta

The thermodynamic properties of $BaCeO_3$ at temperatures from 5 to 940 K

M.J. Scholten [a,*], J. Schoonman [a], J.C. van Miltenburg [b], E.H.P. Cordfunke [c]

[a] *Laboratory for Applied Inorganic Chemistry, Delft University of Technology, Julianalaan 136, NL-2628 BL Delft, Netherlands*

[b] *Department of Interfaces and Thermodynamics, Utrecht University, Padualaan 8, NL-3584 CH Utrecht, Netherlands*

[c] *Netherlands Energy Research Foundation ECN, P.O. Box 1, NL-1755 ZG Petten, Netherlands*

Received 4 August 1994; accepted 11 April 1995

Abstract

Low-temperature heat capacities of $BaCeO_3$ have been measured from 5 to 370 K by adiabatic calorimetry, and the high-temperature enthalpy increments have been measured from 510 to 940 K by drop calorimetry. From the results, smoothed thermodynamic functions have been tabulated at selected temperatures up to 1500 K. For the standard molar entropy of $BaCeO_3$, the value $S^\circ(298.15\ K) = (144.5 \pm 0.3)\ J\ K^{-1}\ mol^{-1}$ has been found.

Keywords: Adiabatic; $BaCeO_3$; Drop calorimetry; Heat capacity; Thermodynamics

1. Introduction

Solid solutions based on the perovskite-type oxide barium cerate have been explored for use in solid oxide fuel cells and high-temperature hydrogen sensors [1].

Thermodynamic properties are required in order to evaluate the chemical stability of $BaCeO_3$ in different environments, for instance in an atmosphere containing CO_2 [2,3].

From e.m.f. measurements, Levitskii et al. calculated the standard Gibbs energy and enthalpy of formation from the oxides between 1200 and 1400 K [4]. Very recently,

* Corresponding author. Present address: Leeststraat 13, NL-1825 JL Alkmaar, Netherlands.

SSDI 0040-6031(95)02431-X

Gopalan and Virkar [5] calculated the Gibbs energy of the reaction $BaCO_3(s) + CeO_2(s) \rightarrow BaCeO_3(s) + CO_2(g)$ from e.m.f. measurements. The standard molar enthalpy of formation at 298.15 K has been measured by Morss and Mensi [6] and Goudiakas et al. [7] by solution calorimetry.

In this study the low-temperature heat capacities were measured by adiabatic calorimetry [8], and the high-temperature enthalpy-increments by drop calorimetry [9]. The derived thermodynamic properties are presented.

2. Experimental

$BaCeO_3$ was prepared by heating a stoichiometric mixture of $BaCO_3$ and CeO_2 (Cerac) in air at 1323–1373 K. X-ray diffraction analysis revealed no second phase.

The low-temperature heat capacities were measured by adiabatic calorimetry. The calorimeter used and its measuring system were described previously [10]. A sample mass of 12.140 g was loaded into the calorimeter corresponding to 0.037303 mol (based on a molar mass of 325.44 g mol^{-1}) and the calorimeter was closed with an annealed gold gasket under a pressure of 1000 Pa of helium. Minor recent improvements in the apparatus were described in an article on 2-chloronaphthalene [11]. Measurements were started at 5 K. The temperature drift during the stabilization periods did not indicate any metastability of the sample.

The enthalpy increments above 510 K were measured in an isothermal diphenylether drop calorimeter, as described in detail previously [12]. For the measurements, the samples were enclosed in spherical quartz ampoules with a volume of approximately 3.6 cm^3. The ampoules were heated in a furnace, the temperature of which was measured with a calibrated platinum-to-platinum/10 mass% rhodium thermocouple to ± 0.1 K. After thermal equilibration, the ampoule was dropped into the calorimeter, where the energy of the ampoule and the sample melted diphenyl ether in equilibrium with its liquid in a closed system. The resulting volume increase of the ether was determined by weighing the displaced mercury. The ratio of energy input to the mass of mercury displaced was a constant for the apparatus, and was obtained by calibration with NIST (formerly NBS) standard reference material (No. 720) synthetic sapphire, Al_2O_3. Details of the calorimeter, calibration, and performance are given in Ref. [12]. For the present measurements, 6.97905 g of $BaCeO_3$ was enclosed in a quartz ampoule of mass 1.17657 g. Loading of the ampoule was performed in an argon-filled glove box, and all masses were corrected for weighing in argon. A correction was made to account for the difference in enthalpy between the calorimeter temperature (300 K), and the standard reference temperature, using C_p°(298.15 K) values from the present low-temperature measurements.

3. Results and discussion

The experimental low-temperature molar heat capacities are given in Table 1. These results were used to calculate the derived thermodynamic properties as given in

Table 1
Experimental heat capacities of $BaCeO_3$

T/K	$C_p^{\ominus}$/(J mol^{-1} K^{-1})	T/K	$C_p^{\ominus}$/(J mol^{-1} K^{-1})	T/K	$C_p^{\ominus}$/(J mol^{-1} K^{-1})	T/K	$C_p^{\ominus}$/(J mol^{-1} K^{-1})
Series I		49.19	28.30	168.32	90.31	305.31	112.48
6.55	0.20	52.32	30.86	172.35	91.49	308.78	112.83
8.97	0.26	55.52	33.56	176.38	92.65	312.49	113.11
10.27	0.42	58.79	36.20	180.43	93.72	316.19	113.48
11.66	0.62	62.12	38.78	184.47	94.73	Series V	
13.32	1.03	65.51	41.19	188.52	95.71	315.19	113.46
14.85	1.81	68.96	43.67	192.59	96.59	318.21	113.71
16.46	2.53	72.35	45.98	196.64	97.43	321.28	113.91
18.22	3.37	75.59	47.07	200.70	98.14	324.35	114.18
20.11	4.49	78.68	50.27	204.76	98.96	327.41	114.48
22.09	5.83	81.63	52.18	208.81	99.76	330.46	114.76
24.17	7.42	84.49	53.96	212.85	100.49	333.52	114.93
26.35	9.14	87.25	55.60	216.86	101.21	336.59	115.25
28.65	10.90	89.94	57.31	220.85	101.91	339.65	115.48
30.84	12.53	92.55	58.81	224.82	102.54	342.71	115.69
32.72	14.04	95.10	60.20	228.78	103.19	345.77	115.93
Series II		97.60	61.59	232.71	103.79	348.83	116.13
8.90	0.19	Series IV		236.64	104.42	351.89	116.35
10.87	0.53	102.91	64.88	240.54	104.99	354.95	116.58
12.34	0.68	105.69	66.33	244.43	105.55	358.02	116.72
13.99	1.40	109.02	68.00	248.31	106.12	361.08	116.85
15.65	2.10	112.90	70.03	252.17	106.65	364.14	117.04
17.37	2.87	116.78	71.90	256.02	107.15	367.21	117.26
19.26	3.97	120.67	73.66	259.86	107.65	370.28	117.44
21.23	5.20	124.57	75.34	263.68	108.13	373.34	117.53
23.29	6.74	128.50	76.90	267.50	108.59		
25.46	8.49	132.43	78.39	271.30	109.00		
27.74	10.18	136.38	79.81	275.09	109.51		
30.12	12.06	140.33	81.19	278.87	109.93		
Series III		144.30	82.57	282.64	110.34		
35.11	16.52	148.29	83.94	286.40	110.73		
37.69	18.74	152.27	85.28	290.15	111.21		
40.29	20.99	156.27	86.59	293.89	111.40		
43.19	23.46	160.28	87.88	297.62	111.86		
46.16	25.72	164.30	89.13	301.35	112.24		

Table 2. Between $T = 0$ and 10 K, the relation

$$C_p^{\circ} = 3.8 \times 10^{-4} (T^3/K^3)\ \text{J mol}^{-1}\ \text{K}^{-1}$$

was used. From 10 K upwards, the experimental heat capacities were interpolated and the derived thermodynamic properties were calculated by numerical integration. The molar heat capacity at 298.15 K was calculated to be $C_p^{\circ}(298.15\ \text{K}) = (111.9 \pm 0.2)$ J mol^{-1} K^{-1}, and the absolute entropy at 298.15 K, $S^{\circ}(298.15\ \text{K}) = (144.5 \pm 0.3)$ J mol^{-1} K^{-1}.

Table 2
Low-temperature thermodynamic functions of $BaCeO_3$

T/K	$C_p^{\ominus}$/(J mol^{-1} K^{-1})	$S^{\ominus}$/(J mol^{-1} K^{-1})
10	0.38080	0.12555
20	4.4233	1.3386
30	11.965	4.5148
40	20.736	9.1376
50	28.959	14.650
60	37.166	20.662
70	44.399	26.939
80	51.134	33.266
90	57.345	39.652
100	63.082	45.979
120	73.367	58.434
140	81.075	70.349
160	87.801	81.624
180	93.621	92.291
200	98.028	102.44
220	101.77	111.91
240	104.93	120.89
260	107.67	129.46
280	110.08	137.52
298.15	111.91	144.51
300	112.08	145.17
320	113.83	152.49
340	115.49	159.39
360	116.82	166.04

The high-temperature molar enthalpy increments are given in Table 3. Using the ECN programme "Enthal", the following polynomial was obtained (298.15–925 K)

$$[H^{\circ}(T) - H^{\circ}(298.15K)] = 121.309T + 6.21327 \times 10^{-3}T^2 + 11.6486 \times 10^{5}T^{-1} - 40627.6 \text{ J mol}^{-1}$$

The results of the enthalpy increment measurements are presented graphically in Fig. 2 in an $[H^{\circ}(T) - H^{\circ}(298.15\text{ K})]/(T - 298.15)$ versus T plot, together with the low-temperature data. The high-temperature data join smoothly with the low-temperature data.

The smoothed thermodynamic quantities of $BaCeO_3$ at selected temperatures from 298.15 to 1500 K are listed in Table 4. The formation properties were calculated from the enthalpy of formation of $BaCeO_3$: $\Delta_f H^{\circ}(298.15\text{ K}) = -(1686.5 \pm 3.9)$ kJ mol^{-1} [7]. This value has been recommended by Goudiakas et al. [7], and was obtained by weighing the results of measurements by Morss and Mensi [6] and Goudiakas et al. [7]. Auxiliary data for the reference states of barium, cerium and oxygen were taken from Barin [13].

Table 3
Experimental enthalpy increments of $BaCeO_3$

T/K	$[H^{\ominus}(T) - H^{\ominus}(298.15\,K)]$/(J mol^{-1})		Deviation %
	Exp.	Calc.	
507.6	24802	24845	−0.17
537.8	28424	28576	−0.53
577.5	33453	33518	−0.19
599.7	36352	36298	0.15
629.2	40071	40011	0.15
661.0	44038	44035	0.01
721.7	51916	51771	0.28
752.9	55851	55775	0.14
784.3	59629	59822	−0.32
815.6	63840	63873	−0.05
847.4	68110	68006	0.15
888.8	73502	73411	0.12
928.4	78318	78606	−0.37
940.9	80415	80251	0.20

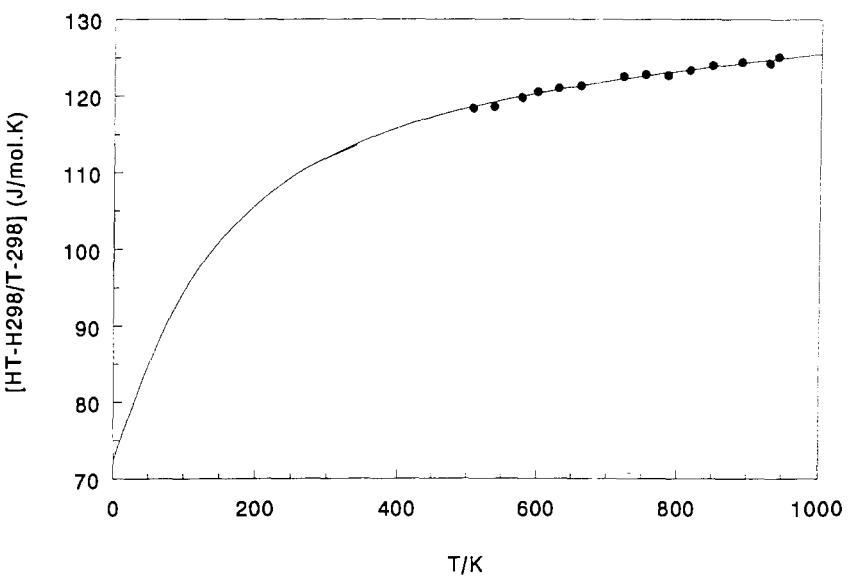

Fig. 1. The reduced enthalpy increments of $BaCeO_3$.

Levitskii et al. [4] calculated the standard Gibbs energy of formation of $BaCeO_3$ from the oxides BaO and CeO_2 at 1200 and 1400 K from e.m.f. measurements. In their calculation, they have used for the standard Gibbs energy of the reaction $BaO + CaF_2 \rightarrow BaF_2 + CaO$, the following values: $\Delta G^{\circ}(1200\,K) = -45100\,J\,mol^{-1}$, and

Table 4
High-temperature thermodynamic functions of $BaCeO_3$

T/K	$C_p^\ominus$/(J mol^{-1} K^{-1})	$S^\ominus$/(J mol^{-1} K^{-1})	$[G^\ominus(T)-H^\ominus(298.15)]/T$/(J mol^{-1} K^{-1})	$[H^\ominus(T)-H^\ominus(298.15)]$/(J mol^{-1})	$\Delta_f H^\ominus(T)$/(J mol^{-1})	$\Delta_f G^\ominus(T)$/(J mol^{-1})
298.15	111.910	144.510	−144.510	0	−1686500	−1598520
300	112.094	145.203	−144.512	207	−1686476	−1597974
400	118.999	178.513	−149.007	11802	−1685087	−1568685
500	122.863	205.514	−157.694	23910	−1684278	−1539698
600	125.529	228.162	−167.602	36336	−1684465	−1510771
700	127.630	247.675	−177.679	48997	−1683702	−1481891
800	129.430	264.838	−187.523	61852	−1683430	−1453082
900	131.055	280.178	−196.981	74878	−1683130	−1424306
1000	132.571	294.065	−206.006	88060	−1685891	−1395559
1100	134.016	306.769	−214.597	101389	−1699053	−1365620
1200	135.412	318.490	−222.772	114861	−1698819	−1335317
1300	136.774	329.382	−230.559	128471	−1698428	−1305042
1400	138.112	339.568	−237.985	142215	−1697931	−1274799
1500	139.431	349.141	−245.080	156092	−1697345	−1244594

$\Delta G^\circ(1400\ \text{K}) = -44800\ \text{J mol}^{-1}$, as obtained from the thermodynamic tables of Glushko (1981).

Replacing these values with $\Delta G^\circ(1200\ \text{K}) = -58139\ \text{J mol}^{-1}$, and $\Delta G^\circ(1400\ \text{K}) = -57879\ \text{J mol}^{-1}$ from Barin [13], and using the $\Delta_f G^\circ$ data of BaO and CeO_2 from Barin [13], the values $\Delta_f G^\circ(1200\ \text{K}) = -1337997\ \text{J mol}^{-1}$, and $\Delta_f G^\circ(1400\ \text{K}) = -1277504\ \text{J mol}^{-1}$ are obtained for the standard Gibbs energy of formation of $BaCeO_3$ from the elements. These values differ by 0.2% from our extrapolated measurements. A third law evaluation of these measurements at 1200 and 1400 K gives the enthalpy of formation at 298.15 K of $-1689.2\ \text{kJ mol}^{-1}$ for *both* temperatures. Values for $[G^\circ(T) - H^\circ(298.15)]/T$ of BaO and CeO_2, and values for $\Delta_f H^\circ(298.15\ \text{K})$ of BaO and CeO_2 were taken from Barin [13]. This third-law enthalpy is in good agreement with the calorimetric value, $-(1686.5 \pm 3.9)\ \text{kJ mol}^{-1}$ [7].

In Fig. 3, the $\log pCO_2$ versus $1/T$ relationships for the equilibria $BaO + CO_2 \rightleftarrows BaCO_3$, and $BaCeO_3 + CO_2 \rightleftarrows BaCO_3 + CeO_2$ are presented. For the latter equilibrium, three different sources of data have been used. These equilibrium lines are calculated using the data of Levitskii et al. [4], this study, Gopalan and Virkar [5], and also data for BaO, $BaCO_3$, CeO_2, and CO_2 from Barin [13]. TG-DTA data from Scholten et al. [2] have also been included in the plot. A hysteresis was observed in the temperatures of the thermal and gravimetric effects in the heating and cooling curve for the 50% $BaCO_3$–50%CeO_2 mixture in CO_2. Our calculated line falls within the temperature range obtained by the TG-DTA measurements.

As can be seen from Fig. 3, the slope of the line of Gopalan and Virkar [5] differs from all other lines. They calculated this line from data obtained by e.m.f. measure-

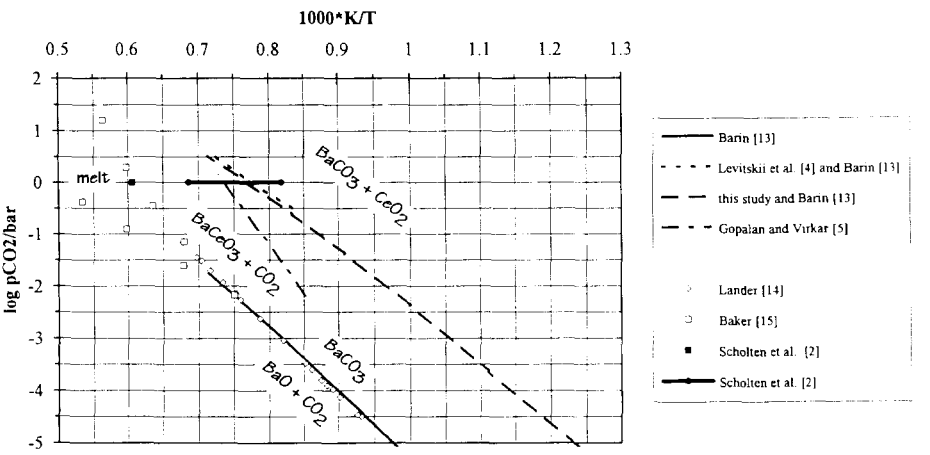

Fig. 2. Stabilities of BaO and $BaCeO_3$ in CO_2-containing atmosphere.

ments of the following galvanic cell:

$$CO_2,O_2|BaCO_3 + BaF_2 + Pt|BaF_2|BaCeO_3 + CeO_2 + BaF_2 + Pt|CO_2,O_2.$$

The temperature range studied was 1173–1373 K ($1000/T = 0.85 - 0.73\ K^{-1}$), and a flow of CO_2 at $\sim$ 1.2 atm ($\log pCO_2/bar = 0.085$) was passed over the galvanic cell. They assumed the half-cell electrode reactions to be:

left: $BaCO_3 + 2F^- \rightarrow BaF_2 + CO_2 + 0.5O_2 + 2e^-$

right: $BaF_2 + CeO_2 + 0.5O_2 + 2e^- \rightarrow BaCeO_3 + 2F^-$

and the overall (potential determining) reaction to be:

$$BaCO_3 + CeO_2 \rightarrow BaCeO_3 + CO_2$$

A third-law evaluation of these measurements at 1100, 1200, 1300 and 1400 K gives the enthalpies of formation at 298.15 K of -1646.5, -1657.9, -1669.8 and -1682.2 kJ mol^{-1}, respectively. Values for $[G^\circ(T) - H^\circ(298.15)]/T$ of CO_2, $BaCO_3$, and CeO_2, and values for $\Delta_f H^\circ(298.15\ K)$ of CO_2, $BaCO_3$, and CeO_2 were taken from Barin [13]. These third-law enthalpies deviate significantly from the calorimetric value of $-(1686.5 \pm 3.9)$ kJ mol^{-1} [7], and also show a large temperature dependence. Therefore, we believe that the cell reaction does not attain thermodynamic equilibrium, which indicates that $BaCeO_3$ is unstable in a CO_2 environment in the temperature regime used by Gopalan and Virkar [5]. The solid electrolyte BaF_2 as used by Gopalan and Virkar [5] was prepared by sintering BaF_2 powder in air at 1273 K for 4 h, which probably results in the formation of oxygen-contaminated BaF_2 [16]. The reaction with oxygen can be expressed as

$$0.5O_2(g) + 2F_F^x \rightarrow OF_F' + V_F^\bullet + F_2(g).$$

Here, the Kröger–Vink defect notation is used. F_F^x represents a regular fluoride ion on a fluoride lattice site. The effective charge is zero (x). O_F' represents an oxide ion on

a fluoride lattice site with an effective charge of $-q(')$, and $V_F^{\cdot}$ denotes a fluoride ion vacancy with an effective charge of $+q(\cdot)$. This oxygen-contaminated BaF_2 can lead to the redox reaction

$$O_F' + 0.5O_2(g) + V_F^{\cdot} + 2e'$$

because oxide ions are mobile in BaF_2 via the fluoride ion vacancies. This redox reaction may occur next to the previously mentioned half-cell reactions as given by Gopalan and Virkar [5], and influence the cell potential.

Acknowledgements

The authors acknowledge R.R. van der Laan (ECN) for the drop calorimetry measurements and Dr. A. Goossens (TUD) for his comments on the manuscript.

References

[1] H. Iwahara, in M. Balkanski, T. Takahashi and H.L. Tuller (Eds.), Solid State Ionics, Elsevier, 1992, pp. 575–586.
[2] M.J. Scholten, J. Schoonman, J.C. van Miltenburg and H.A.J. Oonk, Solid State Ionics, 61 (1993) 83–91.
[3] M.J. Scholten, J. Schoonman, J.C. van Miltenburg and H.A.J. Oonk, in S.C, Singhai and H. Iwahara (Eds.), Proceedings of the Third International Symposium on Solid Oxide Fuel Cells, The Electrochemical Society Proceedings 93–4, Pennington (1993), pp. 146–155.
[4] V.A. Levitskii, S.L. Sorokina, Yu.Ya. Skolis and M.L. Kovba, Inorg. Mater., 21 (1986) 1190–1193.
[5] S. Gopalan and A.V. Virkar, J. Electrochem. Soc., 140 (1993) 1060–1065.
[6] L.R. Morss and N. Mensi, in G.J. McCarthy, H.B. Silber and J.J. Rhyne (Eds.), The Rare Earths in Modern Science and Technology, Plenum Press, New York, 1982, pp. 279–282.
[7] J. Goudiakas, R.G. Haire and J. Fuger, J. Chem. Thermodyn., 22 (1990) 577–587.
[8] E.F. Westrum, Jr., G.T. Furukawa and J.P. McCullough, in J.P. McCullough and D.W. Scott (Eds.), Experimental Thermodynamics, Vol. I, Calorimetry on Non-Reacting Systems, Butterworths, London, 1968, pp. 133–214.
[9] T.B. Douglas and E.G. King, in J.P. McCullough and D.W. Scott (Eds.), Experimental Thermodynamics, Vol. I, Calorimetry on Non-Reacting Systems, Butterworths, London, 1968, pp. 293–331.
[10] J.C. van Miltenburg, G.J.K. van den Berg and M.J. van Bommel, J. Chem. Thermodyn., 19 (1987) 1129–1137.
[11] J.C. van Miltenburg and M.L. Verdonk, J. Chem. Thermodyn., 23 (1991) 273–279.
[12] E.H.P. Cordfunke, R.P. Muis and G. Prins, J. Chem. Thermodyn., 11 (1979) 819.
[13] I. Barin, Thermochemical Data of Pure Substances, VCH, Weinheim, 1989.
[14] J.J. Lander, J. Am. Chem. Soc., 73 (1951) 5794.
[15] E.H. Baker, J. Chem. Soc., (1964) 699.
[16] K.E.D. Wapenaar and J. Schoonman, J. Solid State Chem., 25 (1978) 31–37.